Temporal coherence after multiple forward scattering through random three-dimensional inhomogeneities in an ocean waveguide

Tianrun Chen
Department of Mechanical Engineering, Massachusetts Institute of Technology, Cambridge, Massachusetts 02139

Purnima Ratilal
Department of Electrical and Computer Engineering, Northeastern University, Boston, Massachusetts 02115

Nicholas C. Makris
Department of Mechanical Engineering, Massachusetts Institute of Technology, Cambridge, Massachusetts 02139

(Received 23 January 2008; revised 17 June 2008; accepted 22 June 2008)

An analytical expression is derived for the temporal coherence of an acoustic field after multiple forward scattering through random three-dimensional (3D) inhomogeneities in an ocean waveguide. This expression makes it possible to predict the coherence time scale of field fluctuations in ocean-acoustic measurements from knowledge of the oceanography. It is used to explain the time scale of acoustic field fluctuations observed at megameter ranges in various deep ocean-acoustic transmission experiments. It is shown that this time scale is nonlinearly related to the much longer coherence time scale of deep ocean internal waves through a multiple forward scattering process. It is also shown that 3D scattering effects become pronounced when the acoustic Fresnel width exceeds the cross-range coherence length of the deep ocean internal waves, which lead to frequency and range-dependent power losses in the forward field that may help to explain historic long range measurements. © *2008 Acoustical Society of America.* [DOI: 10.1121/1.2967475]

PACS number(s): 43.30.Re [RCG] Pages: 2812–2822

I. INTRODUCTION

Internal waves cause random compressibility and density fluctuations that can have a pronounced accumulated effect on acoustic signals propagating over long ranges in the deep ocean. The resulting random multiple forward scattering causes significant fluctuations in the acoustic field,[1–8] leads to degradation in the temporal coherence of acoustic signals[9–11] and significant signal-dependent noise.[12] Understanding the properties of this signal-dependent noise is often critical to effectively employ acoustics to ocean remote sensing and communication,[13–19] as well as in the Acoustic Thermometry of Ocean Climate (ATOC).[10] Knowledge of the coherence time scale of a received signal is essential in (1) reducing the error of any measurement or estimate obtained from fluctuating acoustic field data by stationary averaging and (2) applying the fundamental coherent processing techniques of ocean acoustics, such as matched filtering, beamforming, matched-field and synthetic aperture processing. The coherence time scale, for example, is needed to determine the number of *statistically independent* samples of the received acoustic signal during a given measurement time, which can then be averaged to reduce estimation error and signal-dependent noise.[12,20] Since coherent processing must typically be restricted to *within* the coherence time scale of field fluctuations, a good estimate of the coherence time scale is usually necessary to design an effective experiment.

In this paper, we derive a general analytical expression for the temporal correlation function, which can be used to predict the coherence time scale of the acoustic power and field propagated through two-dimensional (2D) and three-dimensional (3D) random inhomogeneities, such as internal waves, bubbles, fish schools, eddies, and surface waves. From this expression, the coherence time scale is calculated for acoustic waves propagating through random internal wave inhomogeneities. It is shown that the coherence time scale of the acoustic field fluctuations observed at megameter ranges in various deep ocean-acoustic transmission experiments[10,21] can be explained by multiple forward scattering through linear internal waves in the deep ocean. The roughly 10 min acoustic coherence time scale measured[10,21] is shown to be nonlinearly related to the much longer 4 h coherence time scale of the internal waves. The latter is derived from the Garret–Munk (GM) spectrum.[22,23] Analysis of the temporal coherence function at zero time lag, which corresponds to the expected intensity of the fluctuating signal, shows that 3D scattering from internal waves can lead to power loss in the low frequency long range propagation in the deep ocean. For a given receiver range, these losses begin to become pronounced as the frequency decreases to the point where the Fresnel length[24] of the acoustic measurements exceeds the cross-range coherence length[24] of the internal waves. This leads to out-of-plane scattering that removes energy from the forward direction. After reaching a

maximum, power losses in the forward direction begin to decrease due to weakening Rayleigh–Born scattering as the acoustic frequency decreases. This may explain the unexpected attenuation observed in some historic long range (megameter) low frequency (5–75 Hz) measurements.[1,25]

Much related work in the 1970s and 1980s focused on using ray theory to work toward an estimate of temporal coherence by accumulating random phase fluctuations along isolated water-borne ray paths in the deep ocean.[2,26] Due to perceived oversimplifications, many moved away from ray theory and began performing numerical Monte Carlo simulations with the 2D parabolic wave equation. For example, in Ref. 27, a 2D Monte Carlo approach based on a parabolic approximation for a specific deep ocean environment was used to estimate the temporal coherence function. Some disadvantages of the Monte Carlo approach, however, are that (1) it does not provide a general analytical expression for the temporal coherence function but, instead, requires intensive numerical calculations for each specific case and (2) it is restricted to 2D propagation and scattering scenarios.

In Sec. II, analytical expressions for the temporal correlation functions of the acoustic power and field forward propagated through a slowly time-varying random medium are derived. In Sec. III, the mean and temporal coherence of the scatter function are derived for internal wave inhomogeneities in the deep ocean. This is required to determine the temporal coherence function of the acoustic power and field. Differences between 2D and 3D scattering processes are reviewed in Sec. IV. Illustrative examples are provided in Sec. V.

Before closing the Introduction, it is useful to first briefly review key steps in the derivation by Ratilal and Makris[24] that will also be needed here. Ratilal and Makris[24] combined the waveguide scattering theory and a differential marching procedure analogous to that used in free space optics by Rayleigh to derive the mean and power of the acoustic field forward propagated through 3D random inhomogeneities in terms of waveguide modes. That analysis is for the mean, spatial covariance, and temporal *variance* of the field. Since the temporal coherence function and the coherence time scale require the temporal *covariance*, it must be derived here, since the temporal variance and covariance are only equal at zero time lag. To obtain the temporal covariance, we follow the same marching procedure used in Ref. 24 to calculate the temporal coherence function of the acoustic power and forward field propagated through 3D inhomogeneities. We define the coherence time scale to be the e-folding time at which the temporal coherence function falls to $1/e$ of its zero time lag value. Knowledge of this time scale is often essential for designing underwater experiments.

Since the inhomogeneities are assumed to follow a stationary random process over time, the mean field remains as the time invariant result derived in Ref. 24. The process of propagating through a single differential slab of random inhomogeneities causes a change in the mean acoustic field. For each mode, this change can be expressed as a product of factors including the incident field, a complex modal wavenumber change induced by scattering, and the thickness of the slab. The mean field after multiple forward scattering through the inhomogeneous medium, obtained by integrating over differential slabs, takes the form of a product of the incident field and an exponential factor that involves the accumulated modal wavenumber changes over range from source to receiver. These wavenumber changes determine the dispersive and attenuating effects of the inhomogeneities, through their real and imaginary parts, respectively, and account for mode coupling in the scattering process.

Ratilal and Makris[24] used a similar marching procedure to derive the mean power of the forward field. The incremental change in acoustic power due to a single slab of inhomoegeneities can be expressed in terms of the depth integral of the second moment of the scattered field, as well as cross terms between the scattered and incident fields. This change can then be expressed as the product of the incident power, the difference between modal variance and attenuation coefficients, and slab thickness. Modal variance coefficients, introduced by depth integration of the scattered field second moment, depend on the variance of intrinsic properties of the inhomogeneities, such as compressibility and density. The acoustic power at the receiver range is then obtained by marching the power change equation from the source to the receiver through direct integration. This power is expressed as a product of the incident power and an exponential factor involving the range integration of the difference between the modal variance and attenuation coefficients.

II. ANALYTICAL MODEL FOR TEMPORAL COHERENCE OF THE ACOUSTIC POWER AND FIELD FORWARD PROPAGATED THROUGH A SLOWLY TIME-VARYING RANDOM MEDIUM

In this section, we derive an analytical expression for the temporal correlation function of the acoustic power and field forward propagated through a slowly time-varying random medium based on the normal mode method. We assume that (1) the random medium follows a stationary process and (2) the medium in a single slab is static during the time period of acoustic wave propagation through it. This is a valid assumption since the correlation time scale of medium fluctuation is much longer than the time it takes the acoustic wave to propagate through a single slab. Note that the derivation of the temporal correlation function of acoustic power (depth-integrated temporal correlation of acoustic total field) does not require an assumption of acoustic modal independence.[24] The assumption of modal independence is only used here to estimate the temporal correlation of the forward field at a specified receiver location $\mathbf{r}$. It is approximately valid when the random component of the field becomes a circular complex Gaussian random variable,[12] since the independence of at least a few dominant modes is then necessary by the central limit theorem. Gaussian field fluctuations are typical in many ocean-acoustic measurements.[12]

All the derivations in this section are based on a single frequency transmission. In the Appendix, we extend our model of the temporal correlation function to a narrow-band signal, which can be approximately expressed in terms of the temporal correlation function of the forward field.

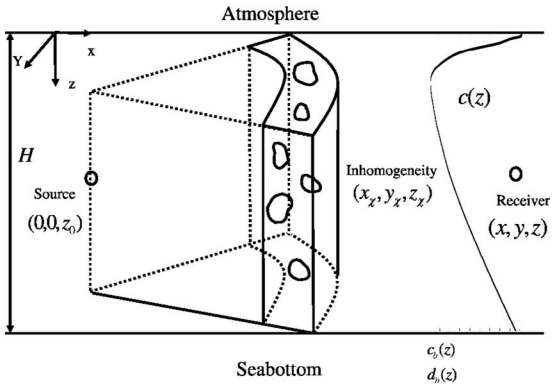

FIG. 1. The geometry of the source, receiver, and inhomogeneities.

A. Mean scattered field for a slowly time-varying random medium

Here, we provide the expression for the mean acoustic field scattered through slowly time-varying random inhomogeneities that are confined within a slab centered at ρ_s of thickness $\Delta\rho_s$.

As shown in Fig. 1, the origin of the coordinate system is placed at the air-water interface with the positive z-axis pointing downward. The source is located at the horizontal origin $\mathbf{r}_0=(0,0,z_0)$, receiver coordinates are given by $\mathbf{r}=(x,y,z)$, and inhomogeneity centers are given by $\mathbf{r}_\chi=(x_\chi,y_\chi,z_\chi)$. Here, t will solely be used to denote time dependence. [The notation t used in Ref. 24 is not for time dependence but denotes target coordinates $\mathbf{r_t}=(x_t,y_t,z_t)$.] Spatial cylindrical (ρ,ϕ,z) and spherical systems (r,θ,ϕ) are defined by $x=r\sin\theta\cos\phi$, $y=r\sin\theta\sin\phi$, $z=r\cos\theta$, and $\rho^2=x^2+y^2$. The horizontal and vertical wavenumber components for the nth mode are, respectively, $\xi_n=k\sin\alpha_n$ and $\gamma_n=k\cos\alpha_n$, where α_n is the elevation angle of the mode measured from the z-axis. Here, $0\le\alpha_n\le\pi/2$ so that the down- and upgoing plane wave components of each mode have elevation angles α_n and $\pi-\alpha_n$, respectively. The corresponding vertical wavenumber of the down- and upgoing components of the nth mode are γ_n and $-\gamma_n$, respectively, where $\Re\{\gamma_n\}\ge 0$. The azimuth angle of the mode is denoted by β. The wavenumber magnitude k equals the angular frequency ω divided by the sound speed c in the object layer, where $k^2=\xi_n^2+\gamma_n^2$. The geometry of spatial and wavenumber coordinates is shown in Fig. 2 of Ref. 28.

The scattered field from random inhomogeneities confined within the slab is found by summing contributions from unit volumes of inhomogeneity as described in Eq. (1) of Ref. 24. The scattered field discussed in the present paper is different from Eq. (1) of Ref. 24, since it varies as a function of time due to the slow *time-varying* random inhomogeneities in the slab according to

$$\Phi_s(\mathbf{r}|\mathbf{r}_0,\Delta\rho_s(\rho_s),f,t)=\int\int\int_{\Delta V_s}\varphi_s(\mathbf{r}|\mathbf{r}_0,\mathbf{r}_\chi,f,t)\mathrm{d}V_\chi, \quad (1)$$

where ΔV_s is the volume of the slab, $\varphi_s(\mathbf{r}|\mathbf{r}_0,\mathbf{r}_\chi,f,t)$ is the scattered field per unit volume of inhomogeneities *centered* at $\mathbf{r}_\chi$, and t is the time at the receiver $\mathbf{r}$.

The scattered field from a unit volume of slowly varying inhomogeneity, which has been derived from Green's theorem in Refs. 29 and 30, can be expressed as

$$\begin{aligned}\varphi_s(\mathbf{r}|\mathbf{r}_0,\Delta\rho_s(\rho_s),f,t)=\sum_{m=1}\sum_{n=1}\frac{(4\pi)^2}{k}[&A_m(\mathbf{r}-\mathbf{r}_\chi)A_n(\mathbf{r}_\chi-\mathbf{r}_0)s_{\mathbf{r}_\chi,t}(\pi-\alpha_m,\beta_s(\phi,\phi_\chi);\alpha_n,\phi_\chi)\\&-B_m(\mathbf{r}-\mathbf{r}_\chi)A_n(\mathbf{r}_\chi-\mathbf{r}_0)s_{\mathbf{r}_\chi,t}(\alpha_m,\beta_s(\phi,\phi_\chi);\alpha_n,\phi_\chi)-A_m(\mathbf{r}-\mathbf{r}_\chi)B_n(\mathbf{r}_\chi-\mathbf{r}_0)\\&\times s_{\mathbf{r}_\chi,t}(\pi-\alpha_m,\beta_s(\phi,\phi_\chi);\pi-\alpha_n,\phi_\chi)+B_m(\mathbf{r}-\mathbf{r}_\chi)B_n(\mathbf{r}_\chi-\mathbf{r}_0)s_{\mathbf{r}_\chi,t}(\alpha_m,\beta_s(\phi,\phi_\chi);\pi-\alpha_n,\phi_\chi)],\end{aligned} \quad (2)$$

where $A_n(\mathbf{r}_\chi-\mathbf{r}_0)$ and $B_n(\mathbf{r}_\chi-\mathbf{r}_0)$ are the amplitudes of the *down-* and *upgoing* modal plane wave components incident on the inhomogeneity at $\mathbf{r}_\chi$ defined in Eqs. (3) and (4) of Ref. 24, $A_m(\mathbf{r}-\mathbf{r}_\chi)$ and $B_m(\mathbf{r}-\mathbf{r}_\chi)$ are the amplitudes of *up-* and *downgoing* modal components scattered from the inhomogeneity defined in Eqs. (5) and (6) of Ref. 24, $\beta_s(\phi,\phi_\chi)=\phi-\arcsin\{\rho_\chi/|\boldsymbol{\rho}-\boldsymbol{\rho}_\chi|\sin(\phi_\chi-\phi)\}$ is the receiver azimuth from the target, and $s_{\mathbf{r}_\chi,t}(\alpha,\beta;\alpha_i,\beta_i)$ is the scatter function density[24] of inhomogeneities at $\mathbf{r}_\chi$.

Assuming that the inhomogeneities obey a stationary process in time, the *mean* scatter function density is time invariant. The mean scattered field from a single inhomogeneous slab can then still be expressed as

$$\begin{aligned}\langle\Phi_s(\mathbf{r}|\mathbf{r}_0,\Delta\rho_s(\rho_s),f,t)\rangle&=\langle\Phi_s(\mathbf{r}|\mathbf{r}_0,\Delta\rho_s(\rho_s),f)\rangle\\&=\sum_n\Phi_i^n(\mathbf{r}|\mathbf{r}_0,f)i\nu_n(\rho_s)\Delta\rho_s,\end{aligned} \quad (3)$$

by following Eq. (59) of Ref. 24, where $\nu_n(\rho_s)$ is the time-invariant change of the complex wavenumber due to scattering from the slab.

B. Marching temporal correlation through a slowly varying random waveguide with difference and integral equations

In this section, a difference equation is derived for the depth-integrated temporal correlation of the total field scattered from inhomogeneities confined within a slab centered at ρ_s. The depth-integrated temporal correlation of the total

field is then marched through the random waveguide to include multiple forward scattering from all inhomogeneities between the source and receiver.

The total field scattered from inhomogeneities within the slab is

$$\Phi(\mathbf{r}|\mathbf{r}_0,\Delta\rho_s(\rho_s),f,t)=\Phi_i(\mathbf{r}|\mathbf{r}_0,f)+\Phi_s(\mathbf{r}|\mathbf{r}_0,\Delta\rho_s(\rho_s),f,t), \tag{4}$$

where

$$\Phi_i(\mathbf{r}|\mathbf{r}_0,f)=4\pi\frac{i}{d(z_0)\sqrt{8\pi}}e^{-i\pi/4}\sum_n u_n(z)u_n(z_0)\frac{e^{i\xi_n\rho}}{\sqrt{\xi_n\rho}} \tag{5}$$

is the incident field expressed in terms of acoustic normal modes.

The mean total field does not depend on t from Eq. (3) and, as in Eq. (83) of Ref. 24, is given by:

$$\begin{aligned}&\langle\Phi_T(\mathbf{r}|\mathbf{r}_0,f,t)\rangle\\&=\langle\Phi_T(\mathbf{r}|\mathbf{r}_0,f)\rangle\\&=4\pi\frac{i}{d(z_0)\sqrt{8\pi}}e^{-i\pi/4}\sum_n u_n(z)u_n(z_0)\frac{e^{i\xi_n\rho}}{\sqrt{\xi_n\rho}}e^{i\int_0^\rho\nu_n(\rho_s)\mathrm{d}\rho_s},\end{aligned} \tag{6}$$

where the addition of an exponential term accounts for the dispersion and attenuation induced by multiple scattering. From Eq. (4), the depth-integrated temporal correlation of the total field can be written as

$$\begin{aligned}&\int_0^\infty\frac{1}{d(z)}\langle\Phi(\mathbf{r}|\mathbf{r}_0,\Delta\rho_s(\rho_s),f,t)\Phi^*(\mathbf{r}|\mathbf{r}_0,\Delta\rho_s(\rho_s),f,t')\rangle\mathrm{d}z\\&=\int_0^\infty\frac{1}{d(z)}|\Phi_i(\mathbf{r}|\mathbf{r}_0,f)|^2\mathrm{d}z\\&+\int_0^\infty\frac{1}{d(z)}(\langle\Phi_i(\mathbf{r}|\mathbf{r}_0,f)\Phi_s^*(\mathbf{r}|\mathbf{r}_0,\Delta\rho_s(\rho_s),f,t')\rangle\\&+\langle\Phi_i^*(\mathbf{r}|\mathbf{r}_0,f)\Phi_s(\mathbf{r}|\mathbf{r}_0,\Delta\rho_s(\rho_s),f,t)\rangle)\mathrm{d}z\\&+\int_0^\infty\frac{1}{d(z)}\langle\Phi_s(\mathbf{r}|\mathbf{r}_0,\Delta\rho_s(\rho_s),f,t)\\&\times\Phi_s^*(\mathbf{r}|\mathbf{r}_0,\Delta\rho_s(\rho_s),f,t')\rangle\mathrm{d}z.\end{aligned} \tag{7}$$

The first term at the right hand side of Eq. (7) is the incident intensity

$$\int_0^\infty\frac{1}{d(z)}|\Phi_i(\mathbf{r}|\mathbf{r}_0,f)|^2\mathrm{d}z=W_i(\boldsymbol{\rho}|\mathbf{r}_0)=\sum_n W_i^{(n)}(\boldsymbol{\rho}|\mathbf{r}_0), \tag{8}$$

where

$$W_i^{(n)}(\boldsymbol{\rho}|\mathbf{r}_0)=\frac{2\pi}{d^2(z_0)}|u_n(z_0)|^2\frac{1}{\boldsymbol{\rho}|\xi_n|}e^{-2\Im\{\xi_n\}\boldsymbol{\rho}}.$$

The second term of Eq. (7) is the depth-integrated cross term arising from the interference between the incident and the scattered field. By inserting the mean scattered field of Eq. (3) into the second term of Eq. (7) and by invoking modal orthogonality

$$\int_0^\infty\frac{1}{d(z)}u_m(z)u_n(z)\mathrm{d}z=\delta_{nm}, \tag{9}$$

integration leads to

$$\begin{aligned}&\int_0^\infty\frac{1}{d(z)}[\langle\Phi_i(\mathbf{r}|\mathbf{r}_0)\Phi_s^*(\mathbf{r}|\mathbf{r}_0,\Delta\rho_s(\rho_s),f,t')\rangle\\&+\langle\Phi_i^*(\mathbf{r}|\mathbf{r}_0)\Phi_s(\mathbf{r}|\mathbf{r}_0,\Delta\rho_s(\rho_s),f,t)\rangle]\mathrm{d}z\\&=\int_0^\infty\frac{1}{d(z)}[\Phi_i(\mathbf{r}|\mathbf{r}_0)\langle\Phi_s^*(\mathbf{r}|\mathbf{r}_0,\Delta\rho_s(\rho_s),f,t')\rangle+\Phi_i^*(\mathbf{r}|\mathbf{r}_0)\\&\times\langle\Phi_s(\mathbf{r}|\mathbf{r}_0,\Delta\rho_s(\rho_s),f,t)\rangle]\mathrm{d}z\\&=-\sum_n W_i^{(n)}(\boldsymbol{\rho}|\mathbf{r}_0)2\Im\{\nu_n(\rho_s)\}\Delta\rho_s.\end{aligned} \tag{10}$$

The last term of Eq. (7) is the depth-integrated temporal correlation of the field scattered from the slab. The temporal correlation of the scattered field $\langle\Phi_s(\mathbf{r}|\mathbf{r}_0,\Delta\rho_s(\rho_s),f,t)\times\Phi_s^*(\mathbf{r}|\mathbf{r}_0,\Delta\rho_s(\rho_s),f,t')\rangle=\mathrm{corr}_{\Phi_s\Phi_s}(\Delta\rho_s(\rho_s),f,\tau=t-t')$ depends on the temporal and spatial correlation of the scatter function density $\langle s_{\mathbf{r}_\chi,t}(\alpha,\beta,\alpha_i,\beta_i)s^*_{\mathbf{r}_{\chi'},t'}(\alpha',\beta',\alpha'_i,\beta'_i)\rangle$, which will be discussed in Sec. II C. When $t=t'$, $\mathrm{corr}_{\Phi_s\Phi_s}(\Delta\rho_s(\rho_s),f,\tau)$ becomes the second moment of the scattered field $\langle|\Phi_s(\mathbf{r}|\mathbf{r}_0,\Delta\rho_s(\rho_s),f)|^2\rangle$ of Eq. (61), Ref. 24. From Sec. III B of Ref. 24, the depth-integrated second moment of the scattered field is

$$\begin{aligned}&\int_0^\infty\frac{1}{d(z)}\langle|\Phi_s(\mathbf{r}|\mathbf{r}_0,\Delta\rho_s(\rho_s),f)|^2\rangle\mathrm{d}z\\&=\sum_{n=1}^\infty W_i^{(n)}(\boldsymbol{\rho}|\mathbf{r}_0)\mu_n(\rho_s,\tau)|_{\tau=0}\Delta\rho_s,\end{aligned} \tag{11}$$

where $\mu_n(\rho_s,0)$ is the variance coefficient that contains a modal sum to account for modal coupling due to the random scattering process. When $t\neq t'$, we can apply the procedure used in the derivation of Eq. (11) to calculate the last term in Eq. (7),

$$\begin{aligned}&\int_0^\infty\frac{1}{d(z)}\langle\Phi_s(\mathbf{r}|\mathbf{r}_0,\Delta\rho_s(\rho_s),f,t)\Phi_s^*(\mathbf{r}|\mathbf{r}_0,\Delta\rho_s(\rho_s),f,t')\rangle\mathrm{d}z\\&=\sum_{n=1}^\infty W_i^{(n)}(\boldsymbol{\rho}|\mathbf{r}_0)\mu_n(\rho_s,\tau=t-t')\Delta\rho_s,\end{aligned} \tag{12}$$

where $\mu_n(\rho_s,\tau)$ is the *temporal* variance coefficient, which accounts for modal coupling and quantifies the modal energy transferred from the mean field to the covariance field. It also describes how the forward field decorrelates as the time lag $\tau=t-t'$ increases after propagating through a slowly time-varying medium. The dependence of $\mu_n(\rho_s,\tau)$ on time lag τ is a consequence of its dependence on the temporal covariance of the scatter function density $\mathrm{cov}_{ss}(\rho_s,z_\chi,z_{\chi'},\tau)$, which will be discussed in Sec. II C.

Inserting Eqs. (8), (10), and (12) into Eq. (7), the depth-integrated temporal correlation of the total field is found to be

$$\int_0^\infty \frac{1}{d(z)}\langle\Phi(\mathbf{r}|\mathbf{r}_0,\Delta\rho_s(\rho_s),f,t)\Phi^*(\mathbf{r}|\mathbf{r}_0,\Delta\rho_s(\rho_s),f,t')\rangle \mathrm{d}z$$
$$= \langle W_T(\boldsymbol{\rho}|\mathbf{r}_0,\tau)\rangle$$
$$= \sum_n W_i^{(n)}(\boldsymbol{\rho}|\mathbf{r}_0)(1+\mu_n(\rho_s,\tau)-2\Im(\nu_n(\rho_s)))\Delta\rho_s. \quad (13)$$

This can be rewritten as a difference equation

$$\Delta\langle W_T(\boldsymbol{\rho}|\mathbf{r}_0,\tau=t-t')\rangle = \sum_n \Delta\langle W_T^{(n)}(\boldsymbol{\rho}|\mathbf{r}_0,\tau)\rangle$$
$$= \sum_n W_i^{(n)}(\boldsymbol{\rho}|\mathbf{r}_0)(\mu_n(\rho_s,\tau)-2\Im(\nu_n(\rho_s)))\Delta\rho_s. \quad (14)$$

Following the marching process described in Sec. III B of Ref. 24, we have

$$\langle W_T(\boldsymbol{\rho}|\mathbf{r}_0,\tau)\rangle = \sum_n \langle W_T^{(n)}(\boldsymbol{\rho}|\mathbf{r}_0,\tau)\rangle$$
$$= \sum_n W_i^{(n)}(\boldsymbol{\rho}|\mathbf{r}_0)e^{\int_0^\rho(\mu_n(\rho_s,\tau)-2\Im\{\nu_n(\rho_s)\})\mathrm{d}\rho_s}. \quad (15)$$

Assuming independence between acoustic modes and following the derivation for the second moment of the forward field in Sec III C of Ref. 24, the temporal correlation of the forward field at receiver $\mathbf{r}$ can be expressed as

$$\langle\Phi(\mathbf{r}|\mathbf{r}_0,f,t)\Phi^*(\mathbf{r}|\mathbf{r}_0,f,t')\rangle$$
$$= \mathrm{corr}_{\Phi\Phi^*}(\mathbf{r}|\mathbf{r}_0,f,\tau)$$
$$= \sum_n |\phi_i^{(n)}(\mathbf{r}|\mathbf{r}_0)|^2 \exp\left(\int_0^\rho [\mu_n(\rho_s,\tau)-2\Im\{\nu_n(\rho_s)\}]\mathrm{d}\rho_s\right), \quad (16)$$

where $|\phi_i^{(n)}|^2$ is the incident intensity of acoustic mode n in a static ocean waveguide. Since both $\mu_n(\rho_s,\tau)$ and $\nu_n(\rho_s)$ depend on the position of inhomogeneities along the acoustic propagation path, range dependence in the scattering process can be taken into account.

C. Complex wavenumber change and temporal covariance coefficient

As explained in Sec. II A, the complex wavenumber change $\nu_n(\rho_s)$ is time independent. The expression for $\nu_n(\rho_s)$ is given in Eq. (60a) of Ref. 24 as

$$\nu_n(\rho_s) = \int_0^\infty \frac{2\pi}{k}\frac{1}{\xi_n}\frac{1}{d(z_t)}[(N_n^{(1)})^2 e^{i2\gamma_{nz_t}}$$
$$\times\langle s_{\mathbf{r}_{\chi',t}}(\pi-\alpha_n,\phi;\alpha_n,\phi)\rangle - N_n^{(2)}N_n^{(1)}$$
$$\times\langle s_{\mathbf{r}_{\chi',t}}(\alpha_n,\phi;\alpha_n,\phi)\rangle - N_n^{(1)}N_n^{(2)}$$
$$\times\langle s_{\mathbf{r}_{\chi',t}}(\pi-\alpha_n,\phi;\pi-\alpha_n,\phi)\rangle$$
$$+ (N_n^{(2)})^2 e^{-i2\gamma_{nz_t}}\langle s_{\mathbf{r}_{\chi',t}}(\alpha_n,\phi;\pi-\alpha_n,\phi)\rangle]\mathrm{d}z_t. \quad (17)$$

At zero time lag, the temporal covariance coefficient $\mu_n(\rho_s,\tau)$ becomes the variance coefficient $\mu_n(\rho_s,\tau=0)$. The variance coefficients for 2D and 3D scattering processes, respectively, are explicitly expressed in Eqs. (74) and (77) of Ref. 24. The variance coefficient contains a term $C_{s,s}(\rho_s,z_\chi,z_{\chi'},m,n)$ found in Eq. (72) of Ref. 24, which is a function of *spatial* correlation of the scatter function density $\mathrm{cov}_{ss}(s_{\rho_s,z_\chi},s_{\rho_s,z_{\chi'}})=\langle s_{\mathbf{r}_\chi}(\alpha,\beta;\alpha_i,\beta_i)s^*_{\mathbf{r}_{\chi'}}(\alpha',\beta';\alpha_i',\beta_i')\rangle$.

For nonzero time lag, the time dependence in $\mu_n(\rho_s,\tau)$ is introduced by the time lag dependent term $C_{s,s}(\rho_s,z_\chi,z_{\chi'},m,n,\tau)$, which is obtained by replacing $\mathrm{cov}_{ss}(s_{\rho_s,z_\chi},s_{\rho_s,z_{\chi'}})$ with $\mathrm{cov}_{ss}(\rho_s,z_\chi,z_{\chi'},\tau)$ in $C_{s,s}(\rho_s,z_\chi,z_{\chi'},m,n)$. The temporal covariance of the scatter function density $\mathrm{cov}_{ss}(\rho_s,z_\chi,z_{\chi'},\tau)$ is derived for 2D and 3D scenarios, respectively, in the following section. Then, we give the expressions of the $\mu_n(\rho_s,\tau)$ by following the derivation of $\mu(\rho_s,\tau=0)$ in Sec. III B of Ref. 24.

1. Inhomogeneities fully correlated within the Fresnel width (2D)

Here, the cross-range coherence length ℓ_y of the random inhomogeneity is greater than the Fresnel width[24] Y_F, which corresponds to an effective 2D scattering process for forward scatter. The spatio-temporal correlation of the scatter function density is given by

$$\langle s_{\mathbf{r}_{\chi',t}}(\alpha,\beta,\alpha_i,\beta_i)s^*_{\mathbf{r}_{\chi',t'}}(\alpha',\beta',\alpha_i',\beta_i')\rangle$$
$$\approx \ell_x(\rho_s,z_\chi,z_{\chi'})[\langle s_{\boldsymbol{\rho}_s,z_{\chi',t}}(\alpha,\beta,\alpha_i,\beta_i)s^*_{\boldsymbol{\rho}_s,z_{\chi',t'}}(\alpha',\beta',\alpha_i',\beta_i')\rangle$$
$$-\langle s_{\boldsymbol{\rho}_s,z_{\chi',t}}(\alpha,\beta,\alpha_i,\beta_i)\rangle\langle s^*_{\boldsymbol{\rho}_s,z_{\chi',t'}}(\alpha',\beta',\alpha_i',\beta_i')\rangle]\delta(x_\chi-x_{\chi'})$$
$$+\langle s_{\boldsymbol{\rho}_s,z_{\chi',t}}(\alpha,\beta,\alpha_i,\beta_i)\rangle\langle s^*_{\boldsymbol{\rho}_s',z_{\chi',t'}}(\alpha',\beta',\alpha_i',\beta_i')\rangle$$
$$= \ell_x(\rho_s,z_\chi,z_{\chi'})\mathrm{cov}_{ss}(\rho_s,z_\chi,z_{\chi'},\tau)\delta(x_\chi-x_{\chi'})$$
$$+\langle s_{\boldsymbol{\rho}_s,z_{\chi',t}}(\alpha,\beta,\alpha_i,\beta_i)\rangle\langle s^*_{\boldsymbol{\rho}_s',z_{\chi',t'}}(\alpha',\beta',\alpha_i',\beta_i')\rangle, \quad (18)$$

where ℓ_x is the coherence length[24] of the random inhomogeneity in the direction of the acoustic propagation. The temporal covariance of the scatter function density

$$\mathrm{cov}_{ss}(\rho_s,z_\chi,z_{\chi'},\tau=t-t')$$
$$= \langle s_{\boldsymbol{\rho}_s,z_{\chi',t}}(\alpha,\beta,\alpha_i,\beta_i)s^*_{\boldsymbol{\rho}_s,z_{\chi',t'}}(\alpha',\beta',\alpha_i',\beta_i')\rangle$$
$$-\langle s_{\boldsymbol{\rho}_s,z_{\chi',t}}(\alpha,\beta,\alpha_i,\beta_i)\rangle\langle s^*_{\boldsymbol{\rho}_s,z_{\chi',t'}}(\alpha',\beta',\alpha_i',\beta_i')\rangle \quad (19)$$

depends only on the time lag $\tau=t-t'$ not on the absolute time t and t' as a consequence of the temporal stationarity assumption for inhomogeneities in the slab.

The temporal variance coefficient only depends on ℓ_x under the 2D scattering scenario

$$\mu_n^{2\mathrm{D}}(\rho_s,\tau) = \sum_m \frac{1}{|\xi_m|}\int_0^\infty \mathrm{d}z_\chi \int_0^\infty \mathrm{d}z_{\chi'}\frac{\ell_x(\rho_s,z_\chi,z_{\chi'})}{\xi_m}$$
$$\times\frac{4\pi^2}{k(z_\chi)k(z_{\chi'})d(z_\chi)d(z_{\chi'})}C_{s,s}(\rho_s,z_\chi,z_{\chi'},m,n,\tau). \quad (20)$$

2. Inhomogeneities uncorrelated within the Fresnel width

Here, $\ell_y < Y_F$ so that inhomogeneities contained within the Fresnel width lead to a 3D scattering process and are uncorrelated. This leads to

$$\begin{aligned}
&\langle s_{\mathbf{r}_\chi,t}(\alpha,\beta,\alpha_i,\beta_i) s^*_{\mathbf{r}_{\chi'},t'}(\alpha',\beta',\alpha_i',\beta_i')\rangle \\
&\quad \approx A_c(\rho_s,z_\chi,z_{\chi'})[\langle s_{\boldsymbol{\rho}_s,z_\chi,t}(\alpha,\beta,\alpha_i,\beta_i) s^*_{\boldsymbol{\rho}_s,z_{\chi'},t'}(\alpha',\beta',\alpha_i',\beta_i')\rangle \\
&\quad - \langle s_{\boldsymbol{\rho}_s,z_\chi,t}(\alpha,\beta,\alpha_i,\beta_i)\rangle\langle s^*_{\boldsymbol{\rho}_s,z_{\chi'},t'}(\alpha',\beta',\alpha_i',\beta_i')\rangle]\delta(\boldsymbol{\rho}_\chi-\boldsymbol{\rho}_{\chi'}) \\
&\quad + \langle s_{\boldsymbol{\rho}_s,z_\chi,t}(\alpha,\beta,\alpha_i,\beta_i)\rangle\langle s^*_{\boldsymbol{\rho}_s',z_{\chi'},t'}(\alpha',\beta',\alpha_i',\beta_i')\rangle \\
&\quad = A_c(\rho_s,z_\chi,z_{\chi'})\mathrm{cov}_{ss}(\rho_s,z_\chi,z_{\chi'},\tau)\delta(\boldsymbol{\rho}_\chi-\boldsymbol{\rho}_{\chi'}) \\
&\quad + \langle s_{\boldsymbol{\rho}_s,z_\chi,t}(\alpha,\beta,\alpha_i,\beta_i)\rangle\langle s^*_{\boldsymbol{\rho}_s',z_{\chi'},t'}(\alpha',\beta',\alpha_i',\beta_i')\rangle, \qquad (21)
\end{aligned}$$

where $A_c(\rho_s,z_\chi,z_{\chi'})$ is the coherence area of the inhomogeneities.[24]

The temporal covariance is a function of $A_c(\rho_s,z_\chi,z_{\chi'})$ under the 3D scattering scenario

$$\begin{aligned}
\mu_n^{3\mathrm{D}}(\rho_s,\tau) = \sum_m \sqrt{\frac{\rho}{2\pi\xi_m\rho_s(\rho-\rho_s)}}\frac{1}{|\xi_m|}\int_0^\infty \mathrm{d}z_\chi \int_0^\infty \mathrm{d}z_{\chi'} \\
\times A_c(\rho_s,z_\chi,z_{\chi'})\frac{4\pi^2}{k(z_\chi)k(z_{\chi'})d(z_\chi)d(z_{\chi'})} \\
\times C_{s,s}(\rho_s,z_\chi,z_{\chi'},m,n,\tau). \qquad (22)
\end{aligned}$$

In summary, the spatio-temporal correlation of the scatter function density $\langle s_{\mathbf{r}_\chi,t}(\alpha,\beta;\alpha_i,\beta_i) \times s^*_{\mathbf{r}_{\chi'},t'}(\alpha',\beta';\alpha_i',\beta_i')\rangle$ is expressed as a function of the temporal covariance of the scatter function density $\mathrm{cov}_{ss}(\rho_s,z_\chi,z_{\chi'},\tau)$, which accounts for slow time variations of inhomogeneities via time lag τ.

III. STATISTICS OF THE SCATTER FUNCTION DENSITY OF INTERNAL WAVE INHOMOGENEITIES IN A DEEP OCEAN ENVIRONMENT

In this section, we derive expressions for the mean and temporal correlation of the scatter function density when the random inhomogeneities are internal waves in a deep ocean environment. The scatter function density for a coherent volume of internal wave inhomogeneity centered at the horizontal location $\boldsymbol{\rho}_s$ is expressed in terms of the compressibility fraction Γ_κ and the density fraction Γ_ρ by applying the Rayleigh–Born approximation to Green's theorem, as shown in Sec. B of Ref. 31,

$$\begin{aligned}
s_{\boldsymbol{\rho}_s,z_\chi,t}(\alpha,\beta,\alpha_i,\beta_i) = \frac{1}{A_c(\rho_s,z_\chi)}\int\int_{A_c}\frac{k^3}{4\pi}[\Gamma_\kappa(\boldsymbol{\rho}_\chi,z_\chi,t) \\
+ \eta(\mathbf{k},\mathbf{k}_i)\Gamma_d(\boldsymbol{\rho}_\chi,z_\chi,t)]e^{i(\xi_i-\xi)\cdot\mathbf{u}_\chi}\mathrm{d}^2\mathbf{u}_\chi, \qquad (23)
\end{aligned}$$

where $\boldsymbol{\rho}_\chi=\boldsymbol{\rho}_s+\mathbf{u}_\chi$ and $\eta(\mathbf{k},\mathbf{k}_i)=\mathbf{k}_i\cdot\mathbf{k}/k^2=\cos\alpha_i\cos\alpha+\sin\alpha_i\sin\alpha\cos(\beta_i-\beta)$ is the cosine of the angle between the incident and scattered plane wave directions.

The mean scatter function density is

$$\begin{aligned}
\langle s_{\boldsymbol{\rho}_s,z_\chi,t}(\alpha,\beta,\alpha_i,\beta_i)\rangle &= \frac{1}{A_c(\rho_s,z_\chi)}\int\int_{A_c}\frac{k^3}{4\pi}\langle\Gamma_\kappa(\boldsymbol{\rho}_\chi,z_\chi,t) \\
&\quad + \eta(\mathbf{k},\mathbf{k}_i)\Gamma_d(\boldsymbol{\rho}_\chi,z_\chi,t)\rangle e^{i(\xi_i-\xi)\cdot\mathbf{u}_\chi}\mathrm{d}^2\mathbf{u}_\chi \\
&= \frac{1}{A_c(\rho_s,z_\chi)}\frac{k^3}{4\pi}\langle\Gamma_\kappa(\boldsymbol{\rho}_\chi,z_\chi,t) \\
&\quad + \eta(\mathbf{k},\mathbf{k}_i)\Gamma_d(\boldsymbol{\rho}_\chi,z_\chi,t)\rangle\int\int_{A_c} e^{i(\xi_i-\xi)\cdot\mathbf{u}_\chi}\mathrm{d}^2\mathbf{u}_\chi \qquad (24)
\end{aligned}$$

and the temporal correlation of the scatter function is

$$\begin{aligned}
&\langle s_{\boldsymbol{\rho}_s,z_\chi,t}(\alpha,\beta,\alpha_i,\beta_i) s^*_{\boldsymbol{\rho}_s,z_{\chi'},t'}(\alpha',\beta',\alpha_i',\beta_i')\rangle \\
&\quad = \frac{1}{A_c(\rho_s,z_\chi)A_c(\rho_s,z_{\chi'})}\int\int_{A_c}\int\int_{A_c'} e^{i(\xi_i-\xi)\cdot(\mathbf{u}_\chi-\mathbf{u}_{\chi'})} \\
&\qquad \times \mathrm{cov}_{\mathcal{F}\mathcal{F}}(\boldsymbol{\rho}_\chi,\boldsymbol{\rho}_{\chi'},z_\chi,z_{\chi'},t,t')\mathrm{d}^2\mathbf{u}_\chi\mathrm{d}^2\mathbf{u}_{\chi'}, \qquad (25)
\end{aligned}$$

where

$$\begin{aligned}
&\mathrm{cov}_{\mathcal{F}\mathcal{F}}(\boldsymbol{\rho}_\chi,\boldsymbol{\rho}_{\chi'},z_\chi,z_{\chi'},t,t') \\
&\quad = \left(\frac{k^3}{4\pi}\right)^2\langle[\Gamma_\kappa(\boldsymbol{\rho}_\chi,z_\chi,t)+\eta(\mathbf{k},\mathbf{k}_i)\Gamma_d(\boldsymbol{\rho}_\chi,z_\chi,t)] \\
&\quad \times[\Gamma_\kappa(\boldsymbol{\rho}_{\chi'},z_{\chi'},t')+\eta(\mathbf{k},\mathbf{k}_i)\Gamma_d(\boldsymbol{\rho}_{\chi'},z_{\chi'},t')]\rangle \qquad (26)
\end{aligned}$$

is the spatio-temporal correlation of intrinsic scattering properties. To calculate Eqs. (24) and (25), the statistical moments of fractional changes in compressibility Γ_κ and density Γ_d are required.

Since the fluctuations of the sound speed (Δc) and density (Δd) arising from random internal waves are much smaller than the unperturbed or local equilibrium sound speed and density, the fractional change of compressibility Γ_κ and density Γ_d can be expanded up to second order in Taylor series

$$\begin{aligned}
\Gamma_\kappa &\approx \left[-\frac{2\Delta c}{c_0}-\frac{\Delta d}{d_0}\right]+\left[3\left(\frac{\Delta c}{c_0}\right)^2+\left(\frac{\Delta d}{d_0}\right)^2+2\frac{\Delta c\Delta d}{c_0 d_0}\right], \\
\Gamma_d &\approx \frac{\Delta d}{d_0}-\left(\frac{\Delta d}{d_0}\right)^2. \qquad (27)
\end{aligned}$$

Fluctuations of the sound speed and density, for practical purposes, are linearly dependent on the displacement of the internal wave[2,32] $\xi(\boldsymbol{\rho}_\chi,z_\chi,t)$ via

$$\begin{aligned}
\frac{\Delta c(\boldsymbol{\rho}_\chi,z_\chi,t)}{c_0} &= \xi(\boldsymbol{\rho}_\chi,z_\chi,t)\bar{G}(z_\chi)n^2(z_\chi), \\
\frac{\Delta d(\boldsymbol{\rho}_\chi,z_\chi,t)}{d_0} &= \xi(\boldsymbol{\rho}_\chi,z_\chi,t)g^{-1}n^2(z_\chi), \qquad (28)
\end{aligned}$$

where $\bar{G}(z_\chi)$ is a function of the potential temperature and salinity,[2] g is the gravitational constant, and $n(z_\chi)$ is the buoyancy frequency or *Brunt–Väisälä* frequency

$$n^2(z_\chi) = -gd^{-1}\frac{\partial d_p(z_\chi)}{\partial z_\chi}, \tag{29}$$

where $d_p(z_\chi)$ is the potential density.[2]

The displacement ξ of internal waves at location $(\boldsymbol{\rho}_\chi, z_\chi)$ and time t is taken to be a zero-mean Gaussian random variable[2]

$$\xi(\boldsymbol{\rho}_\chi, z_\chi, t) = \sum_j \int H(\boldsymbol{\sigma}, j) W_j(\sigma, z_\chi) \exp(i[\boldsymbol{\sigma}\cdot\boldsymbol{\rho}_\chi - \Omega(\sigma, j)t])\mathrm{d}^2\boldsymbol{\sigma}, \tag{30}$$

where $H(\boldsymbol{\sigma}, j)$ is a zero-mean Gaussian random variable that specifies the jth modal amplitude of internal waves at wave number $\boldsymbol{\sigma}$ and $W_j(\sigma, z_\chi)$ is the jth modal shape of internal waves at depth z_χ. Internal wave angular frequency Ω is related to the magnitude of the internal wave wavenumber σ via the dispersion relation given in Ref. 2.

Assuming that the internal wave field follows a stationary random process in the horizontal space and in time, the spatio-temporal covariance of internal wave displacements at two measurement points $\mathbf{r}_\chi(\boldsymbol{\rho}_\chi, z_\chi)$ and $\mathbf{r}'_\chi(\boldsymbol{\rho}_{\chi'}, z_{\chi'})$ and two times t and t' can be expressed as a function of the horizontal separation $\mathbf{R}=\boldsymbol{\rho}_\chi - \boldsymbol{\rho}'_\chi$ and time lag $\tau = t - t'$;[2,22,23] we have

$$\begin{aligned}\mathrm{cov}_{\xi\xi}(\mathbf{R}, \tau, z_\chi, z_{\chi'}) &= \langle \xi(\boldsymbol{\rho}_\chi, z_\chi, t)\xi(\boldsymbol{\rho}_{\chi'}, z_{\chi'}, t')\rangle \\ &\quad - \langle \xi(\boldsymbol{\rho}_\chi, z_\chi, t)\rangle\langle \xi(\boldsymbol{\rho}_{\chi'}, z_{\chi'}, t')\rangle \\ &= \sum_j \int F_j(\boldsymbol{\sigma}) W_j(\sigma, z_\chi) W_j^*(\sigma, z_{\chi'}) \\ &\quad \times \exp(i[\boldsymbol{\sigma}\cdot\mathbf{R} - \omega(\sigma, j)\tau])\mathrm{d}^2\boldsymbol{\sigma}, \end{aligned} \tag{31}$$

where $F_j(\boldsymbol{\sigma}) = \langle |H(\boldsymbol{\sigma}, j)|^2\rangle$ is the GM spectrum of internal waves, whose expressions and parameters can be found in p. 56 of Ref. 2.

After inserting Eq. (28) into Eq. (27), and Eq. (27) into Eq. (26), the spatio-temporal covariance of intrinsic scattering properties becomes

$$\begin{aligned}&\mathrm{cov}_{\mathcal{F}\mathcal{F}}(\boldsymbol{\rho}_\chi, \boldsymbol{\rho}'_\chi, z_\chi, z_{\chi'}, t, t') \\ &= \frac{k^6}{(4\pi)^2} h(z_\chi) h(z_{\chi'}) \langle \xi(\boldsymbol{\rho}_\chi, z_\chi, t)\xi^*(\boldsymbol{\rho}'_\chi, z_{\chi'}, t')\rangle \\ &= \frac{k^6}{(4\pi)^2} h(z_\chi)(z_{\chi'}) \mathrm{cov}_{\xi\xi}(\mathbf{R}, \tau, z_\chi, z_{\chi'}), \end{aligned} \tag{32}$$

where $h(z_\chi) = [2\bar{G}(z_\chi) + (1-\eta)/g]n^2(z_\chi)$.

We approximate the displacements of internal waves at two horizontal positions $\boldsymbol{\rho}_\chi$ and $\boldsymbol{\rho}_{\chi'}$ within the coherence area A_c as being fully correlated[24,31] such that

$$\begin{aligned}&\mathrm{cov}_{\mathcal{F}\mathcal{F}}(\boldsymbol{\rho}_\chi, \boldsymbol{\rho}'_\chi, z_\chi, z_{\chi'}, t, t') \\ &\approx \frac{k^6}{(4\pi)^2} h(z_\chi) h(z_{\chi'}) \mathrm{cov}_{\xi\xi}(0, \tau, z_\chi, z_{\chi'}). \end{aligned} \tag{33}$$

The mean scatter function density is found to be proportional to the second moment of the internal wave displacement from Eqs. (24), (27), and (30), such that Eq. (19) becomes

$$\begin{aligned}&\mathrm{cov}_{ss}(\rho_s, z_\chi, z_{\chi'}, \tau) \\ &\approx \langle s_{\boldsymbol{\rho}_s, z_\chi, t}(\alpha, \beta, \alpha_i, \beta_i) s^*_{\boldsymbol{\rho}_s, z_{\chi'}, t'}(\alpha', \beta', \alpha'_i, \beta'_i)\rangle. \end{aligned} \tag{34}$$

This is because the *square* of the mean scatter function density proportional to the fourth power of internal wave displacement, is much smaller than $\langle s_{\boldsymbol{\rho}_s, z_\chi, t} s^*_{\boldsymbol{\rho}_s, z_{\chi'}, t'}\rangle$, which is on the order of the second moment of internal wave displacement.

Equation (34) can be expressed as

$$\begin{aligned}\mathrm{cov}_{ss}(\rho_s, z_\chi, z_{\chi'}, \tau) &\approx \frac{k^6 h(z_\chi) h(z_{\chi'})}{(4\pi)^2 A_c(z_\chi) A_c(z_{\chi'})} \mathrm{cov}_{\xi\xi}(0, \tau, z_\chi, z_{\chi'}) \\ &\quad \times \int\int_{A_c} \int\int_{A'_c} e^{i(\xi_i - \xi)\cdot(\mathbf{u}_\chi - \mathbf{u}_{\chi'})} \mathrm{d}^2\mathbf{u}_\chi \mathrm{d}^2\mathbf{u}'_\chi \end{aligned} \tag{35}$$

by substituting Eq. (31) into Eq. (33), then Eq. (33) into Eq. (25). By replacing $\mathrm{cov}_{ss}(s_{\rho_s, z_\chi}, s_{\rho_s, z_{\chi'}})$ with $\mathrm{cov}_{ss}(\rho_s, z_\chi, z_{\chi'}, \tau)$ in Eq. (72) of Ref. 24, we have

$$\begin{aligned}&C_{s,s}(\rho_s, z_\chi, z_{\chi'}, m, n, \tau) \\ &= u_n(z_\chi) u_n^*(z_{\chi'}) u_m(z_\chi) u_m^*(z_{\chi'}) \mathrm{cov}_{ss}(\rho_s, z_\chi, z'_\chi, \tau), \end{aligned} \tag{36}$$

which leads to $\mu_n(\rho_s, \tau)$ by inserting Eq. (36) into Eq. (20).

A purely real modal horizontal wavenumber change $\nu_n(\rho_s)$ is obtained by substituting the mean scatter function density of Eq. (24) into Eq. (60a) cf. Ref. 24. This only accounts for dispersion but not for attenuation in the mean forward field. Assuming no power loss within the Fresnel region or in the forward direction for a 2D scattering process, the depth-integrated intensity at zero time lag $\langle W_T(\boldsymbol{\rho}|\mathbf{r}_0, \tau = 0)\rangle$ must equal the depth-integrated incident intensity $\Sigma_n W_i^{(n)}$ of Eq. (15). This requires

$$\Im(\nu_n^{2\mathrm{D}}(\rho_s)) = \tfrac{1}{2}\mu_n^{2\mathrm{D}}(\rho_s, \tau = 0). \tag{37}$$

Out-of-plane scattering becomes important in 3D scenarios and leads to power loss in the forward direction, which requires an imaginary part in $\nu_n(\rho_s)$. We apply the waveguide extinction theorem[30,33] to calculate $\Im(\nu_n(\rho_s))$ in Eq. (36) of Ref. 28.

IV. 2D AND 3D SCATTERING PROCESSES

The Fresnel width in cross range[24] is defined to be where the incident and forward scattered fields are highly coherent and have a phase difference of less than $\pi/4$. The Fresnel width, $Y_F(\rho, \rho_s) = \sqrt{[\lambda(\rho - \rho_s)\rho_s]/\rho}$, depends on the range of the source, receiver, and scatterer,[24,31] where λ is the acoustic wavelength. The maximum Fresnel width[24,31] $Y_{F_{\max}}(\rho, \rho_s) = \sqrt{\lambda\rho/4}$ occurs at the midpoint between the source and the receiver. When $Y_F < \ell_y$, an internal wave inhomogeneity is correlated within the Fresnel width, which leads to an effective 2D scattering process.

As the receiver range increases, Y_F exceeds ℓ_y, 3D scattering initiates, and uncorrelated internal-wave inhomogene-

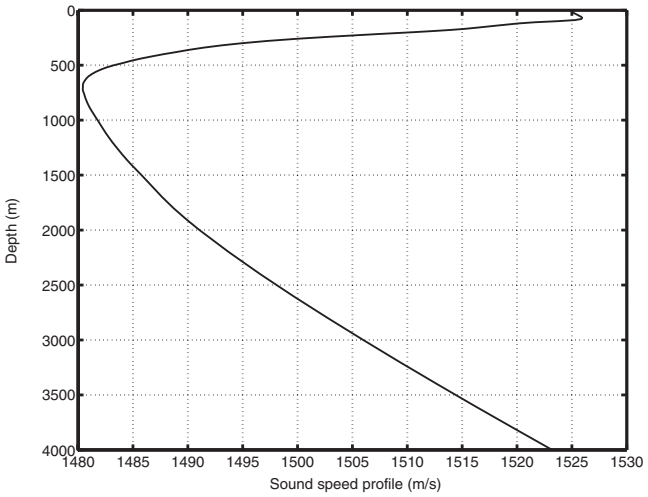

FIG. 2. Representative sound speed profile for the Pacific ocean region between latitudes 20°N and 31°N and longitudes 123°W and 154°W. The depth of the sound-channel axis is roughly 700 m.

ities appear within the Fresnel region. This leads to out-of-plane scattering that causes additional power loss in the forward direction.

V. ILLUSTRATIVE EXAMPLES

Here, a water column of $H=4000$ m depth is used to simulate the geometry of a deep ocean waveguide. The bottom sediment half-space is composed of sand with density $d_b=1.9$ g/cm^3 and sound speed $c_b=1700$ m/s. The attenuation coefficients in the water column and bottom are $\alpha=6\times10^{-5}$ dB/λ and $\alpha_b=0.8$ dB/λ, respectively. A point source transmits acoustic waves at a frequency of 75 Hz. Both the source and the point receiver are located at a depth of 1000 m. We use a sound speed profile calculated from the historical temperature and salinity data[10] corresponding to the Pacific ocean region between latitudes 20 °N and 31 °N and longitudes 123 °W and 154 °W, as shown in Fig. 2.

The temporal correlation function of internal wave displacements at the depth of the sound channel axis is shown in Fig. 3 following Eq. (31). The e-folding correlation time scale of the internal wave field is seen to be approximately 4 h at that depth. As the water depth increases, the coherence time scale of internal waves also increases because internal wave displacements decrease. The temporal correlation of the depth-integrated intensity and the acoustic forward field are shown in Fig. 4 following Eqs. (15) and (16), respectively. Uncertainty in the internal wave energy level leads to variations in the e-folding correlation time scale of the depth-integrated intensity and the forward scattered acoustic field. At three typical GM internal wave energy levels, for example, the e-folding correlation time scales vary between 7 and 14 min, as also shown in Fig. 4. These time scales are more than an order of magnitude smaller than that of the internal waves. Scattering from a single slab containing internal waves causes only a small change in the temporal correlation of the depth-integrated intensity. This is due to the weak scattering from a single slab and the very long time scale of the internal waves with respect to acoustic travel

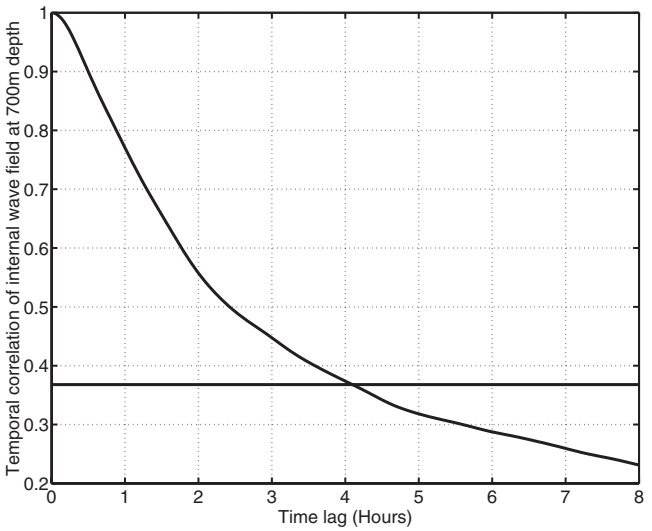

FIG. 3. Temporal correlation function of the internal-wave displacement at 700 m as a function of time lag. The temporal correlation is the *normalized* spatio–temporal covariance of Eq. (28) at zero horizontal separation. The e-folding coherence time is approximately 4 h. The solid horizontal line is plotted at the correlation function value $1/e$.

time through the slab. As acoustic power, or the depth-integrated intensity, is propagated through a series of uncorrelated slabs of inhomogeneities over range, *accumulated* multiple scattering dramatically degrades temporal correlation. This leads to coherence time scales for the acoustic power and forward field that are much shorter than that of the internal wave field. An assumption of modal independence is not required to obtain the temporal correlation and the time scale of the acoustic power.

Acoustic power loss due to scattering is

$$\mathrm{PL}(\boldsymbol{\rho}|\mathbf{r}_0) = 10\log\langle W_T(\boldsymbol{\rho}|\mathbf{r}_0,\tau=0)\rangle - 10\log W_i(\boldsymbol{\rho}|\mathbf{r}_0), \tag{38}$$

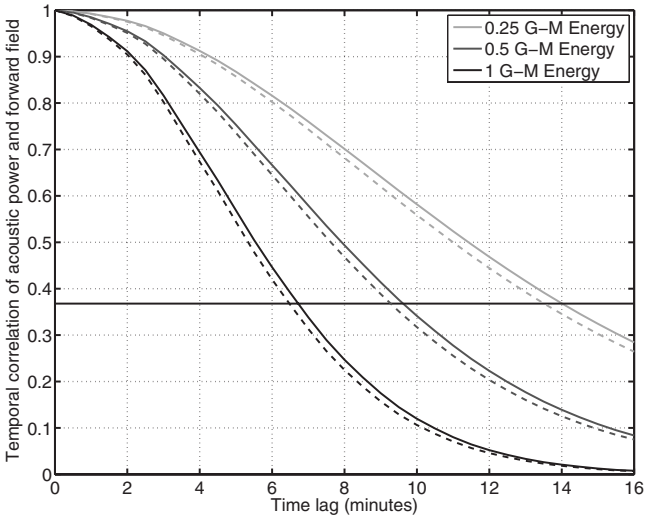

FIG. 4. Temporal correlation function of acoustic power and forward field for 3250 km source-receiver separation as a function of time lag for various possible GM energy levels. The temporal correlations of acoustic power and forward field are the *normalized* temporal covariances of Eqs. (17) and (18), respectively. The e-folding coherence time varies between 7 and 14 min depending on the internal wave energy level. The temporal correlation functions of the acoustic power and forward field are plotted with dashed and solid lines, respectively. The solid horizontal line is plotted at the correlation function value $1/e$.

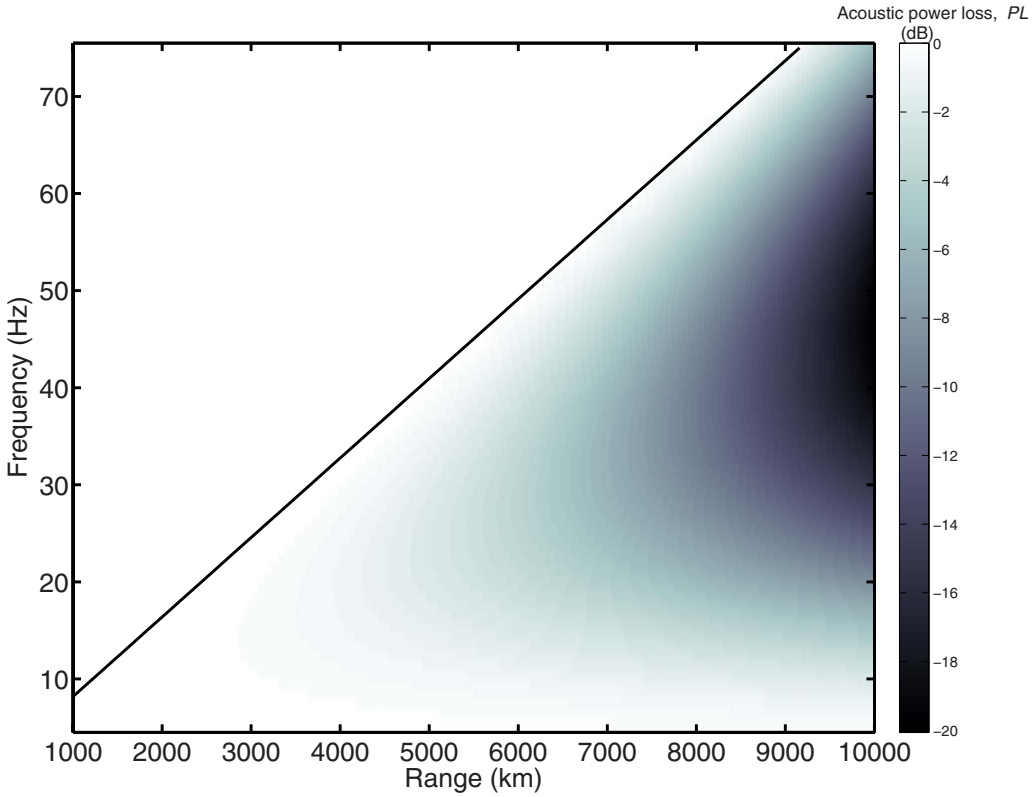

FIG. 5. (Color online) Total acoustic power loss in forward propagation through deep ocean random internal waves as a function of frequency and the source-receiver separation from Eq. (38). The 2D scattering region, $\ell_y > Y_F$, is above the black line and the 3D scattering region, $\ell_y < Y_F$, is below the black line.

where $\langle W_T(\boldsymbol{\rho}|\mathbf{r}_0, \tau=0)\rangle$ is the total acoustic power of Eq. (15) at zero time lag and $W_i(\boldsymbol{\rho}|\mathbf{r}_0)$ is the incident acoustic power of Eq. (8). We plot the acoustic power loss as a function of receiver range and acoustic frequency in Fig. 5. The 2D and 3D scattering regions are separated by a black line showing where $(Y_F)_{\max} = \ell_y$. In the 2D region, there is no power loss in the forward direction, as assumed in Sec. IV. In the 3D region, power loss monotonically increases with source-receiver separation for fixed frequencies. At a given source-receiver separation, however, power loss reaches a maximum in the low frequency regime. This is because two competing factors determine the total power loss: Y_F and $\mu_n^{3D}(\rho_s, 0)$. As frequency decreases, Y_F becomes larger leading to more uncorrelated internal wave inhomogeneities in the Fresnel region. This leads to more out-of-plane scattering and power loss. However, the f^{-6} Rayleigh–Born scattering roll-off for any individual inhomogeneity results in an $f^{-2.5}$ roll-off in variance coefficient $\mu_n(\rho_s, 0)$ at zero time lag, as seen in Eq. (15). This leads to less power loss.

VI. CONCLUSIONS

We have derived an analytical expression for the temporal covariance of the depth-integrated intensity or the acoustic power propagated through 3D random inhomogeneities, from which the coherence time scale of field or power fluctuations can be determined. Knowledge of the coherence time scale is typically essential in ocean-acoustic remote sensing. This is because it determines (1) the number of fluctuations in a given measurement period, which determines the amount of error reduction possible by stationary averaging in any ocean-acoustic remote sensing measurement, and (2) the time window within which the coherent processing essential to ocean-acoustic remote sensing, such as matched filtering, beamforming, matched field processing, and synthetic aperture processing, can be conducted. We have provided a general and rapid way of estimating the coherence time scale to aid in the design of ocean-acoustic experiments and the interpretation of experimental measurements. We show by analysis that the time scale of acoustic power fluctuations after megameter range propagation through internal waves in the deep ocean is roughly 10 min, which matches experimental measurements, and is more than an order of magnitude smaller than the 240 min correlation time scale of the internal wave field. This discrepancy between the acoustic and internal wave time scales is explained by the present theory as the accumulated effect of multiple forward scattering through internal waves on acoustic waves.

We find that power loss due to 3D scattering from internal wave inhomogeneities becomes pronounced when the Fresnel width exceeds the cross-range correlation length of internal waves. As source-receiver separation increases, the Fresnel width increases and contains more uncorrelated internal wave inhomogeneities, which leads to a monotonic increase in power loss. For a given source-receiver separation and decreasing frequency, power loss first increases as the internal wave incoherence accumulates within the Fresnel width, and then decreases due to weakening Rayleigh–Born scattering for any individual inhomogeneity. This may explain the unexpectedly high attenuations historically observed below 100 Hz.[1,25]

APPENDIX: TEMPORAL COHERENCE OF NARROW-BAND ACOUSTIC SIGNALS

Here we discuss extension of the single-frequency transmission of the main text to narrow-band signals. Let the acoustic signal measured at a receiver be

$$\Psi(r|r_0,t) = \Psi_i(r|r_0,t) + \Psi_s(r|r_0,t), \tag{A1}$$

where $\Psi_i(r|r_0,t) = \int_{-\infty}^{\infty} Q(f)\Phi_i(r|r_0,f)e^{-i2\pi ft}df$ is the incident field, $\Psi_s(r|r_0,t) = \int_{-\infty}^{\infty} Q(f)\Phi_s(r|r_0,f,t)e^{-i2\pi ft}df$ is the scattered field, and $Q(f)$ is the source spectrum. The temporal coherence or autocorrelation function of the acoustic signal is

$$\begin{aligned}\langle \Psi(r|r_0,t)\Psi^*(r|r_0,t')\rangle &= \int_{-\infty}^{\infty}\int_{-\infty}^{\infty} Q(f)Q(f') \\ &\times \langle \Phi(r|r_0,f,t)\Phi(r|r_0,f',t')\rangle \\ &\times e^{-i2\pi(ft-f't')}\mathrm{d}f\mathrm{d}f'. \end{aligned}\tag{A2}$$

In order to evaluate Eq. (A2), we need to calculate the temporal correlation of the total field $\langle \Phi(r|r_0,f,t)\Phi^*(r|r_0,f',t')\rangle$ at two different frequencies f and f'.

Derivations for the depth-integrated second moment of the scattered field in Sec. IV B of Ref. 24 and the second term of Eq. (7) in Sec. II B of the present paper rely on modal orthogonality

$$\int_0^{\infty} \frac{1}{d(z)} u_m(f,z)u_n(f,z)\mathrm{d}z = \delta_{nm}. \tag{A3}$$

It can be shown by the numerical simulations that modal orthogonality is still approximately valid for the acoustic modes at two different frequencies f and f' via

$$\int_0^{\infty} \frac{1}{d(z)} u_m(f,z)u_n(f',z)\mathrm{d}z \approx \delta_{nm}, \tag{A4}$$

if the difference between f and f' is smaller than a few Hertz. Consequently, $\langle \Phi(r|r_0,f,t)\Phi^*(r|r_0,f',t')\rangle$ can be approximated as $\langle \Phi(r|r_0,f,t)\Phi^*(r|r_0,f,t')\rangle$ of Eq. (16) for sufficient narrow-band signals satisfying Eq. (A4). Equation (A2) is then approximately

$$\begin{aligned}&\langle \Psi(r|r_0,t)\Psi^*(r|r_0,t')\rangle \\ &\approx |Q(\bar{f})\Delta f|^2 \langle \Phi(r|r_0,\bar{f},t)\Phi^*(r|r_0,\bar{f},t')\rangle e^{-i2\pi\bar{f}(t-t')}, \end{aligned}\tag{A5}$$

where $\bar{f}$ and Δf are the central frequency and bandwidth of the narrow-band signal, respectively.

[1] R. J. Urick, *Sound Propagation in the Sea* (Department of Defense, Arlington, VA, 1979).
[2] R. Dashen, W. H. Munk, K. M. Watson, F. Zachariasen, and S. M. Flatte, *Sound Transmission Through a Fluctuating Ocean* (Cambridge University Press, Cambridge, 1979).
[3] R. P. Porter, R. C. Spindel, and R. J. Jarfee, "Acoustic-internal wave interaction at long ranges in the ocean," J. Acoust. Soc. Am. **56**, 1426–1436 (1974).
[4] W. H. Munk and F. Zachariasen, "Sound propagation through a fluctuating stratified ocean: Theory and observation," J. Acoust. Soc. Am. **59**, 818–838 (1976).
[5] F. Dyson, W. Munk, and B. Zetler, "Interpretation of multipath scintillation Eleuthera to Bermuda in terms of internal waves and tides," J. Acoust. Soc. Am. **59**, 1121–1133 (1976).
[6] J. L. Spiesberger and P. F. Worcester, "Fluctuations of resolved acoustic multipaths at long range in the ocean," J. Acoust. Soc. Am. **70**, 565–576 (1981).
[7] R. P. Porter and R. C. Spindel, "Low-frequency acoustic fluctuations and internal gravity waves in the ocean," J. Acoust. Soc. Am. **60**, 943–958 (1977).
[8] Y. J. F. Desaubies, "On the scattering of sound by internal waves in the ocean," J. Acoust. Soc. Am. **64**, 1460–1469 (1978).
[9] K. D. Heaney, P. N. Mikhalevsky, H. Freese, and W. A. Kuperman, "Internal wave effects on single-frequency coherence, matched field processing, and adiabaticity," J. Acoust. Soc. Am. **103**, 2751 (1998).
[10] P. F. Worcester, B. D. Cornuelle, M. A. Dzieciuch, W. H. Munk, B. M. Howe, J. A. Mercer, R. C. Spindel, J. A. Colosi, K. Metzger, T. G. Birdsall, and A. B. Baggeroer, "A test of basin-scale acoustic therometry using a large aperture vertical array at 3250-km range in the eastern North Pacific Ocean," J. Acoust. Soc. Am. **105**, 3185–3201 (1999).
[11] S. M. Flatte and G. Rovner, "Calculations of internal-wave-induced fluctuations in ocean-acoustic propagation," J. Acoust. Soc. Am. **108**, 526–534 (2000).
[12] N. C. Makris, "The effect of saturated transmission scintillation on ocean acoustic intensity measurements," J. Acoust. Soc. Am. **100**, 769–783 (1996).
[13] N. C. Makris, P. Ratilal, D. Symonds, S. Jagannathan, S. Lee, and R. Nero, "Fish population and behavior revealed by instantaneous continental-shelf-scale imaging," Science **311**, 660–663 (2006).
[14] R. N. Baer and M. D. Collins, "Source localization in the presence of internal waves," J. Acoust. Soc. Am. **118**, 3117–3121 (2005).
[15] P. Ratilal, Y. Lai, D. T. Symonds, L. A. Ruhlmann, J. R. Preston, E. K. Scheer, M. T. Garr, C. W. Holland, J. A. Goff, and N. C. Makris, "Long range acoustic imaging of the continental shelf environment: The Acoustic Clutter Reconnaissance Experiment 2001," J. Acoust. Soc. Am. **117**, 1977–1998 (2004).
[16] N. C. Makris, P. Ratilal, M. Zanolin, and I. Bertsatos, "Obtaining optimal time-delay, source localization and tracking estimates in free space and in an ocean waveguide," J. Acoust. Soc. Am. **116**, 2606 (2004).
[17] K. Yoo and T. C. Yang, "Broadband source localization in shallow water in the presence of internal waves," J. Acoust. Soc. Am. **106**, 3255–3269 (1999).
[18] N. C. Makris, "Optimizing shallow-water sound-speed estimation using parameter resolution bounds," J. Acoust. Soc. Am. **96**, 3234–3235 (1994).
[19] J. L. Spiesberger, "Remote sensing of western boundary currents using acoustic tomography," J. Acoust. Soc. Am. **86**, 346–351 (1989).
[20] E. Naftali and N. C. Makris, "Necessary conditions for a maximum likelihood estimate to become asymptotically unbiased and attain the Cramer–Rao Lower Bound. Part I. General approach with an application to time-delay and Doppler shift estimation," J. Acoust. Soc. Am. **110**, 1917–1930 (2001).
[21] R. E. Williams and H. F. Battestin, "Time coherence of acoustic signals transmitted over resolved paths in the deep ocean," J. Acoust. Soc. Am. **59**, 312–328 (1976).
[22] C. Garrett and W. Munk, "Space-time scales of ocean internal waves," Geophys. Fluid Dyn. **2**, 225–264 (1972).
[23] C. Garrett and W. Munk, "Space-time scales of internal waves:a progress report," J. Geophys. Res. **80**, 291–297 (1975).
[24] P. Ratilal and N. C. Makris, "Mean and covariance of the forward field propagated through a stratified ocean waveguide with three-dimensional random inhomogeneities," J. Acoust. Soc. Am. **118**, 3532–3559 (2005).
[25] R. H. Mellen, D. G. Browning, and L. Goodman, "Diffusion loss in a stratified sound channel," J. Acoust. Soc. Am. **60**, 1053–1055 (1976).
[26] R. Dashen, S. M. Flatte, and S. A. Reynolds, "Path-integral treatment of acoustic mutual coherence functions for rays in a sound channel," J. Acoust. Soc. Am. **77**, 1716–1792 (1996).
[27] J. L. Spiesberger, F. Tappert, and A. R. Jacobson, "Blind prediction of broadband coherence time at basin scales," J. Acoust. Soc. Am. **114**, 3147–3154 (2003).
[28] N. C. Makris, F. Ingenito, and W. A. Kuperman, "Detection of a submerged object insonified by surface noise in an ocean waveguide," J. Acoust. Soc. Am. **96**, 1703–1724 (1994).
[29] F. Ingenito, "Scattering from an object in a stratified medium," J. Acoust. Soc. Am. **82**, 2051–2059 (1987).

[30]P. Ratilal, "Remote sensing of submerged objects and geomorphology in continental shelf waters with acoustic waveguide scattering," Ph.D. thesis, MIT MA, 2002.
[31]T. Chen, P. Ratilal, and N. C. Makris, "Mean and variance of the forward field propagated through three-dimensional random internal waves in a continental-shelf waveguide," J. Acoust. Soc. Am. **118**, 3560–3574 (2005).
[32]A. E. Gill, *Atmosphere-Ocean Dynamics* (Academic, San Diego, CA, 1982).
[33]P. Ratilal and N. C. Makris, "Extinction theorem for object scattering in a stratified medium," J. Acoust. Soc. Am. **110**, 2924–2945 (2001).